ACTA ASTRONOMICA
Vol. **59** (2009) pp. 255–272

Finding the Brightest Galactic Bulge Microlensing Events with a Small Aperture Telescope and Image Subtraction

D. M. Nataf, K. Z. Stanek

Department of Astronomy, Ohio State University, 140 W. 18th Ave., Columbus, OH 43210
e-mail:(nataf,kstanek)@astronomy.ohio-state.edu

and G. A. Bakos

NSF Fellow, Harvard-Smithsonian Center for Astrophysics, 60 Garden St., Cambridge, MA 02138
e-mail:gbakos@cfa.harvard.edu

Received April 30, 2009

ABSTRACT

Following the suggestion of Gould and Depoy (1998) we investigate the feasibility of studying the brightest microlensing events towards the Galactic bulge using a small aperture (≈ 10 cm) telescope. We used one of the HAT telescopes to obtain 151 exposures spanning 88 nights in 2005 of an $8^\circ\!\!.4\times8^\circ\!\!.4$ FOV centered on $(l,b)=(2.85,-5.00)$. We reduced the data using image subtraction software. We find that such a search method can effectively contribute to monitoring bright microlensing events, as was advocated. Comparing this search method to the existing ones we find a dedicated bulge photometric survey of this nature would fulfill a significant niche at excellent performance and rather low cost. We obtain matches to 7 microlensing events listed in the 2005 OGLE archives. We find several other light curves whose fits closely resemble microlensing events. Unsurprisingly, many periodic variable stars and miscellaneous variable stars are also detected in our data, and we estimate approximately 50% of these are new discoveries. We conclude by briefly proposing Small Aperture Microlensing Survey, which would monitor the Galactic bulge around the clock to provide dense coverage of the highest magnification microlensing events.

Key words: *Techniques: photometric – Gravitational lensing – Stars: variables: general*

1. Introduction

Microlensing has seen an impressive string of firsts since Paczyński (1986) got the field going with a "futuristic" plan to probe the Milky Way's halo: Constraints on MACHOs (Bennett *et al.* 1993); Spectroscopic profiling of faint stars (Lennon *et al.* 1996); Direct measurements of stellar masses (An *et al.* 2002); Extrasolar planets (Bond *et al.* 2004); Terrestrial parallax measurements of a thick-disk brown dwarf (Gould *et al.* 2009).

But even with all these successes, there is still ample discovery space remaining in the field of Galactic microlensing. Exploring an unfulfilled niche, Gould and Depoy (1998) advocated using a small aperture telescope (≈ 65 mm diameter), a $6^\circ \times 6^\circ$ field of view, and difference imaging to study microlensing events towards the Galactic bulge. Such a survey would allow one to observe objects at higher brightness and to observe the entire bulge with a few pointings. Three key scientific advantages were specified: the survey would provide an analog to microlensing studies of M31, it would yield a complete inventory of bright bulge variable stars, and data could be taken at the peaks of extreme magnification microlensing events.

Progress within the field of microlensing along with technological advances have modified the prospects for some of these advantages but not eliminated them. As seen in Table 1, there remains a place for a survey observing the entire Galactic bulge in one or few pointings, at high brightness and high cadence. We obtain the specifications for OGLE, MOA and MPF from Udalski (2003), Sako *et al.* (2008), Bennett and Rhie (2000) and Bennett *et al.* (2007). The preliminary specifications for KMTNet, which will network observations at three different locations for round-the-clock time-series, came from Gaudi *et al.* (2009), Park (2008)[1], and Han (private communication).

Table 1

Microlensing surveys, present and future

Survey	Aperture [m]	Pixels	FOV Square Degrees	Limit. Magn.	Saturation Limit	Cadence (Approx)	Bulge Fields
OGLE-III	1.3	8192×8192	0.58×0.58	$I \approx 19.5$	$I \approx 12$	1/(3 nights)	267
MOA-Cam3	1.8	$10 \times (2K \times 4K)$	1.32×1.65	$I \approx 18.5$	$I \approx 12.5$	5/night	22
HAT 2005 Run	0.11	2048×2048	8.4×8.4	$I \approx 12.5$	$I \approx 8$	1.5/night	1
KMTnet	3×1.6	$4 \times (10K \times 10K)$	2×2	$I \approx 21$	$I \approx 12$	144/(24 hours)	4
MPF	1.1	$\approx 8000 \times 6000$	0.95×0.65	$J \approx 20.5$	–	150/(24 hours)	4
SAMS	3×0.1	4096×4096	11×11	$I \approx 14.5$	$I \approx 8.0$	300/(24 hours)	1

Observational summary of major current and future microlensing surveys. Limiting magnitudes (Limit. Magn.) are for 10% photometric precision, except for MPF where the number cited is for 1% precision. Surveys that are line-separated are proposed future surveys (KMTNet is already funded). The cadence of the HAT2005 run appears anomalously low due to its main project taking up most of the observing time.

[1] *http://www.astronomy.ohio-state.edu/≈microfun/MF1/Talks/Park_KMTNet.pdf*

There are a few surveys of microlensing in M31 building on the pioneering work of Crotts and Tomaney (1996). The Angstrom project has been observing since 2005, and has had its early warning system operational since 2007 (Darnley *et al.* 2007). Novati *et al.* (2009) have also conducted 2 years of observations of M31. Closer to home, Galactic bulge variability surveys have often either been limited in FOV such as the Spitzer-IRAC survey (Ramirez *et al.* 2008) or been optimized to a different range of magnitudes such as OGLE (Soszyński *et al.* 2008).

Meanwhile, in the case of high-magnification microlensing events, networks of amateur observers such as MicroFUN (Gould 2008) refine time series at the peaks, but it is hard to maintain the reliability and consistency that would be obtained from a dedicated and automated survey. Nevertheless, high-magnification microlensing events have blossomed into a very critical subfield of microlensing. In his recent review of the field, Gould (2009a) mentions seven planets already discovered by this method as well as six more whose details are not yet published. The 4th microlensing planet, OGLE-2005-BLG-169, was constrained by observer Doekunn An taking over 1000 observations at the magnification peak after being told of the urgency the night of the event (Gaudi *et al.* 2006). The 5th and 6th microlensing planets, OGLE-2006-BLG-109, were perhaps the first Jupiter-Saturn analog found, and the first multiplanet system found using microlensing. The detail extracted from this event was possible due to observations being taken by twelve observatories at or near the peak (Gaudi *et al.* 2008). It is unfortunate that such good observational support is not currently available to all high-magnification microlensing events. The case for a dedicated, automated and high-cadence survey is evident.

Gould and Depoy (1998) also advocated a broad ($\approx 30''$) PSF. Such a PSF is much less dependent on atmospheric conditions, and would reduce pixelization noise, which falls as the inverse 4th power of the PSF (Gould 1996). This end can now be achieved by software methods rather than hardware methods. For example, the HAT telescopes use a sequence of small pointing steps during the exposure to broaden the PSF (Bakos *et al.* 2004). Another technique employed to broaden the PSF, is to use charge shifting by means of an orthogonal transfer array (Johnson *et al.* 2009).

Motivated by the proposal of Gould and Depoy (1998) and by our results, we encourage development of a Small Aperture Microlensing Survey (SAMS). A generic list of technical and observation specifications of such a survey is included in Table 1.

In this paper we report on the performance of our feasibility study. In Section 2 we provide a synopsis of our observational data set. We summarize our reduction methods in Section 3. In Section 4 we report on our search for both known microlensing events as well as previously undiscovered ones. In Section 5 we comment on the potential to find new variable stars within the bulge, presenting a few examples. We conclude in Section 6.

2. Data

We used one of the HAT telescopes, HAT-9, located on Mauna Kea, Hawaii. A Canon 11 cm diameter f/1.8L lens was used to image onto an Apogee AP10 $2\text{K} \times 2\text{K}$ CCD. The resulting pixel scale is $14''$. A detailed description of the equipment and observing program can be found in Bakos *et al.* (2004).

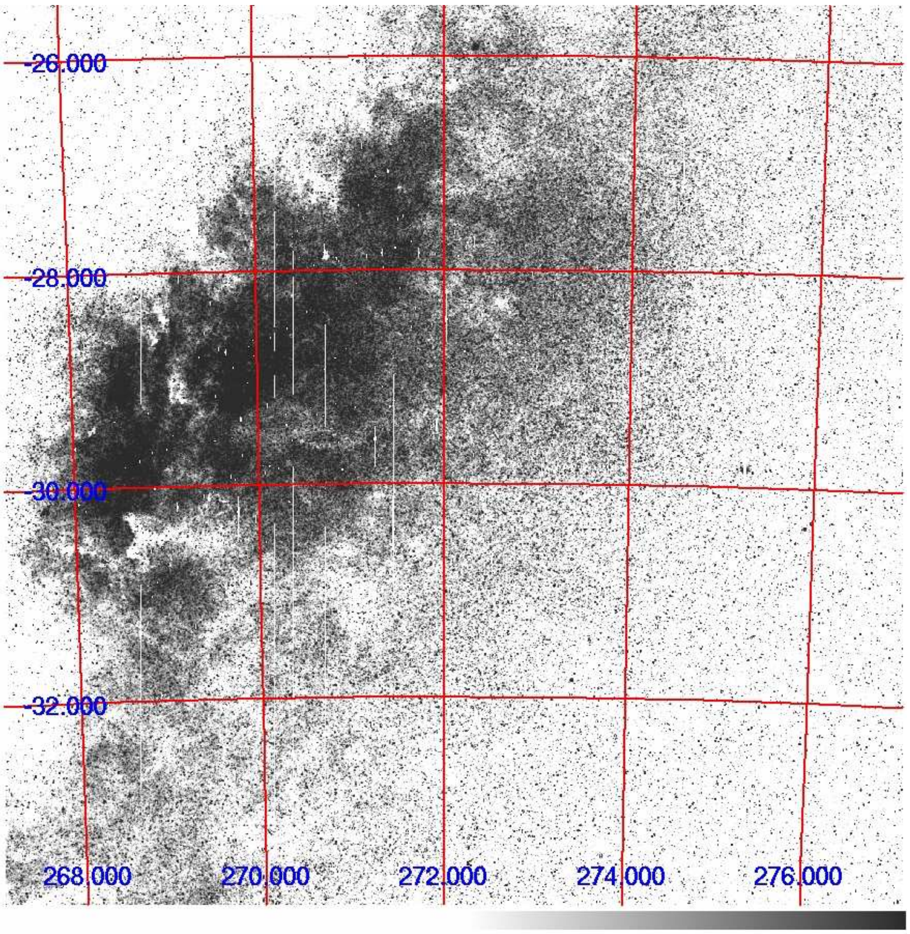

Fig. 1. Image of our field, with $8^{\circ}\!.4 \times 8^{\circ}\!.4$ FOV centered on $(l,b) = (2.85, -5.00)$.

Our observations were taken over an 88 day span between July 22nd and October 18th, 2005, yielding 151 exposures over 61 distinct nights. Our $8^{\circ}\!.4 \times 8^{\circ}\!.4$ FOV is centered on $(\alpha, \delta) = (18^{\mathrm{h}}11^{\mathrm{m}}54^{\mathrm{s}}, -28^{\circ}57'28'')$ (J2000.0), in the general direction of Baade's window, see Fig. 1. Our photometric precision ranges from 1% for the brightest stars ($I \approx 9$ mag) down to 10% at the faint end ($I \approx 13$ mag). Thus, our feasibility study achieved the wide field and the magnitude range necessary to gauge the viability of a dedicated and automated survey, but we did not implemented the high-cadence.

3. Data Reduction

Preliminary CCD reductions such as dark current subtraction and flat-fielding are based on IRAF and discussed in Bakos *et al.* (2004). In subsequent reductions we largely follow the procedure described in Hartman *et al.* (2004), which also dealt with HAT data for a dense stellar field. Key parts and specific changes are discussed below.

3.1. Image Subtraction and Photometry

Due to our $2K \times 2K$ CCD and $\approx 10^5$ sources, we expect a typical source to be within ≈ 7 pixels of another source. However, as can be seen from our reference image (Fig. 1), sources are not evenly distributed and thus we are deep within the domain of dense-field photometry. Additionally, there will be many unresolved stellar sources contributing flux and some sources contributing varying flux throughout our image. To subtract the non-variable components of the images and to obtain light curves of variable objects we use the ISIS package, see Alard and Lupton (1998) and Alard (2000), by now a standard tool when dealing with crowded field variability studies.

Following the usual procedure Hartman *et al.* (2004), we used the image with the best spatial resolution to perform the astrometric calibration step. We then constructed a reference image from 25 of our frames, selecting from frames that had both sharper resolution as well as attempting to have epochs spread throughout the time series. The first condition facilitates reducing the impact of blending on our data, and the second increases the probability that short-duration transient events break our magnitude threshold and show up on succeeding source lists. As the full width at half maximum (FWHM) was generally narrower in the earlier part of the time-series, taking only the sharpest images would have significantly limited the prospects for detecting short-duration transients.

To construct the source list, we used the DAOPHOT/ALLSTAR package (Stetson 1992). Our photometric list is comprised of 115 624 objects – many of them likely to be blends of a number of stars. We then used ISIS to produce the light curves. Fig. 2 shows the light curve RMS *vs.* apparent magnitude for our sources. A few key features can be observed. The "main" sequence of points, which is at approximately lowest RMS for a given magnitude, corresponds to the non-variable sources. There is an intrinsic width due to vignetting. A higher RMS is obtained from fainter sources, as one would expect due to the inverse square-root scaling of photon noise. There is also the impact of the surface brightness of the sky, a significant issue with $14'' \times 14''$ per pixel and when pointed towards the bulge. The sparser population on top with much higher RMS are the candidate variable sources. At the bright end of the distribution, a magnitude precision of 4 millimagnitudes (with 5 minute cadence) is achieved, increasing to 0.1 mag for the fainter objects. This is a demonstration of the prospects for time-series photometry in a dense, wide-field setting using image subtraction.

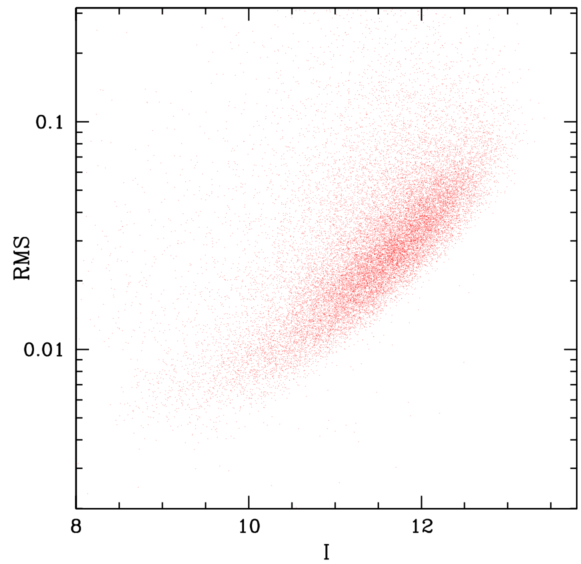

Fig. 2. RMS *vs.* apparent *I*-band magnitude for a representative sample of points.

It is for these same brighter stars that a small-aperture telescope would most contribute to the observational parameter space. 7 714 of the sources have a precision below 10 millimagnitudes, 34 323 have a precision below 20 millimagnitudes and 91 218 have a precision below 50 millimagnitudes.

Magnitude calibrations were done by comparing instrumental magnitudes to *I*-band photometry of all OGLE objects in our field with $I \leq 12.5$ mag, see (Szymański 2005) and (Udalski, Kubiak and Szymański 1997). We then applied a $15''$matching radius to gauge the magnitude shift. Using the median ΔI for the magnitude shift and the upper and lower quartiles to estimate our error, we obtained a shift of (4.6 ± 0.2) magnitudes.

4. Microlensing Analysis

There are currently several groups actively searching for microlensing events towards the Galactic bulge, notably OGLE, MOA, and the MicroFun network. A cursory look at the list of partners in MicroFun[2] reveals the use of equipment ranging in size from 0.25 m (Perth 0.25-m f/6.3 Telescope) to 2.4 m (MDM observatory). At the time of writing, science-grade microlensing detections have rarely been cataloged from data obtained from a telescope whose primary is as small as that of the HAT telescopes – 11 cm. One case identified in the literature is of a 2006 event (Gaudi *et al.* 2008b) which included photometry from the All Sky Automated Survey (ASAS), which uses a ≈ 7 cm diameter primary.

[2] *http://www.astronomy.ohio-state.edu/˜microfun/*

We searched both for the signals of known microlensing events, and also for events not previously discovered.

4.1. Previously Known Microlensing Events

We relied on the OGLE-III Early Warning system's catalog from 2005 (Udalski 2003)[3]. 597 events took place in 2005. We kept those that were within our field of view, that had their peak magnitude within 30 days of our observation window, and that had their peak magnitude above $I \approx 14.5$ mag. The 30 day time frame was a generous match for the typical crossing time, in the hope we might catch the tail end of some events. A peak magnitude of $I \approx 14.5$ mag was used so that the minimum magnitude would yield a signal, as magnitudes below that would wash into noise at our coarse pixelization, low exposure times, and dense sky background. As OGLE's magnitude-sensitivity range is typically between $I \approx 12-19$ mag, this represented some of the brighter OGLE events.

That left us a list of 27 events. Plotting of the light curves for sources centered at the OGLE coordinates yielded seven (visual) confirmations. Of these three are less clear (Fig. 4), and four are of much higher quality (Fig. 3). The visibly clearest events are generally those with larger change in magnitude and higher peak brightness. Due to our low cadence, events with a longer Einstein crossing time were also easier to recognize.

Observational trends manifest themselves in the Figs. 3 and 4. The scatter in the plots drop substantially for the brighter events – which is precisely where one would need lower scatter for a survey such as SAMS, as that would best complement the existing surveys which already have precision photometry for the fainter magnitudes.

We failed to detect many events whose parameters appear as those of the events we did detect or better. For example, BLG-452 had its best fit OGLE curve peak at HJD 2453584.3, with a base magnitude of 19 and a magnification of 8.7 mag. However, the brightest point actually recorded by OGLE corresponded to $I = 18.002$ mag due to the very small period of magnification, and the peak brightness only reached by the fit for a period of hours. While we have three observations on that night, they were within 30 minutes of one another and ≈ 10 hours apart from the estimated time of peak brightness.

4.2. Search for New Microlensing Events

We investigated the possibility of additional microlensing events not previously known. Two different methods were used. The first method was to fit our existing light curves obtained from the DAOPHOT list to microlensing parameters, and the second was to look for events in the sources that did not show up in the DAOPHOT list but did show up in the ISIS abs.fits image, a superposition frame of all the absolute variations from the reference flux.

---

[3]OGLE-III Early Warning System URL: *http://ogle.astrouw.edu.pl/~ogle/ogle3/ews/ews.html*

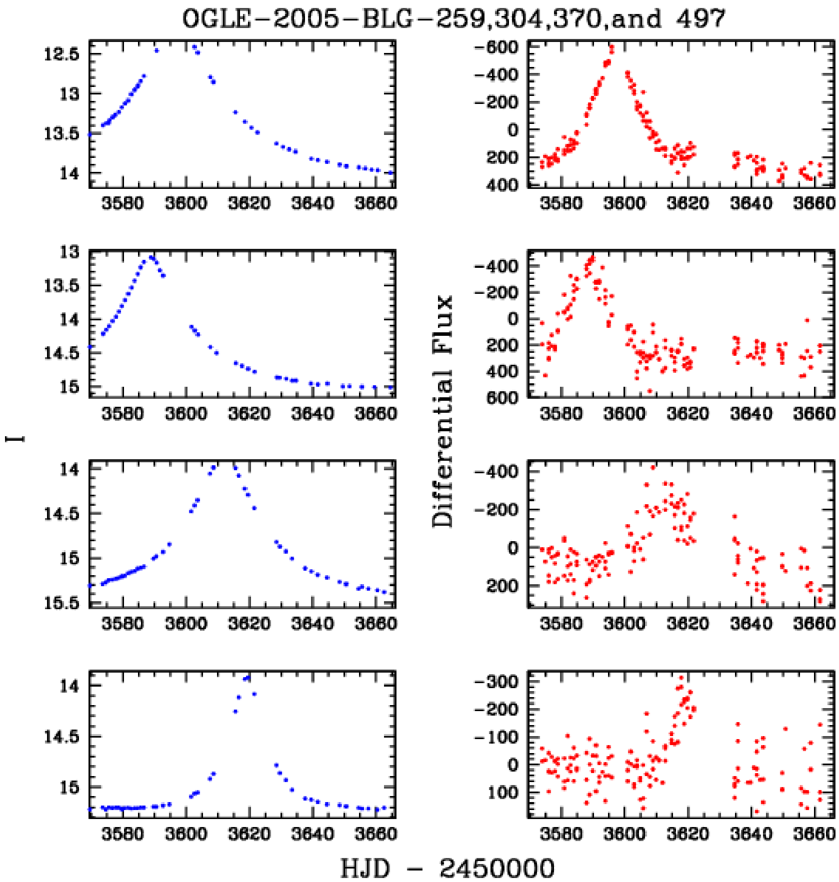

Fig. 3. Plot of known microlensing events with more visually significant matches. The original OGLE light curves are plotted on the *left*, and our matches are plotted on the *right*. Increase in flux displayed as a negative differential count by convention.

Method 1: Using the DAOPHOT *Source List*

To restrict our search to variable stars only we used the J_S coefficient, a measure of correlated variability within specified time windows (Stetson 1996). Sources with a $J_S \geq 2$ were first selected, leaving a list of 9 775 light curves. This selection step immediately removed the possibility of finding any short-duration ($t_e \lesssim$ few days) microlensing events.

With our narrow observational window and low cadence we would not have been able to properly classify such events as microlensing events and not, for example, as dwarf novae.

We fit single-lens microlensing parameters to the light curves using a search and classification algorithm developed by Wyrzykowski *et al.* (2009). We removed light curves with an Einstein crossing time greater than 88 days those with a time of maximum amplification was outside our observational window. We then sorted the light curves by normalized χ^2, and then manually looked at the light curves.

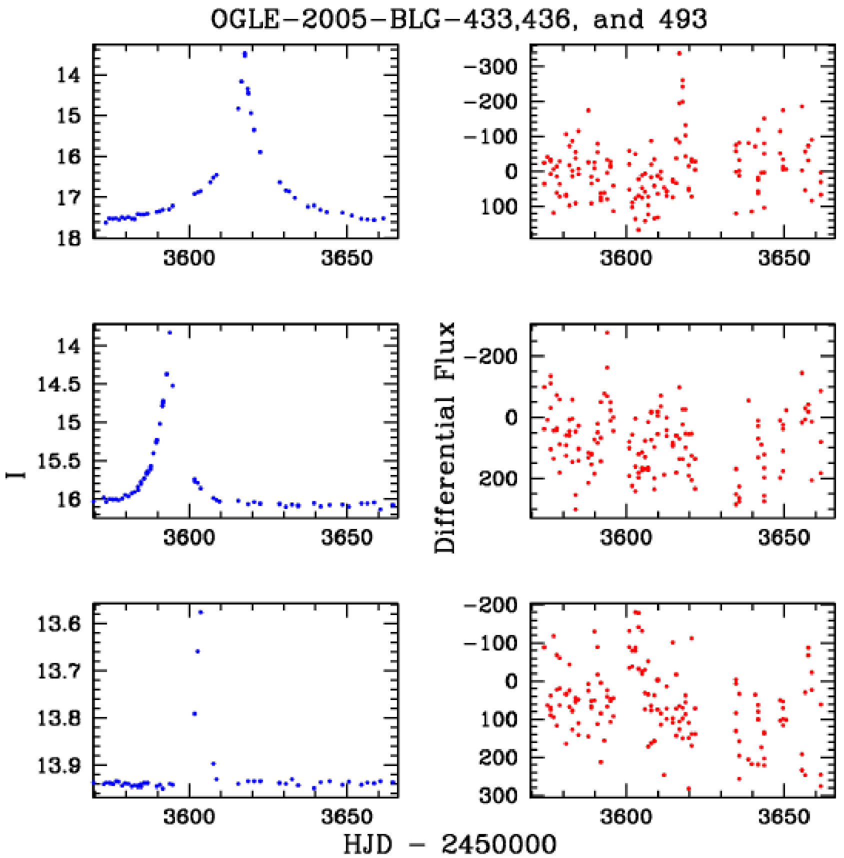

Fig. 4. As in Fig. 3, this time with the three less good microlensing matches.

The best light curves were then refitted with blending allowed to float as a free parameter.

A sample of the best light curves with their microlensing fits are presented in Fig. 5. There were no light curves that we deemed to definitively be microlensing events. Our brief time window does not allow us to comprehensively know which of the sources are normally non-variable. Many of the inherent limitations would whither away in a study with a longer baseline and higher cadence. Of the seven OGLE microlensing events recognized within our data, only one (BLG-259) with J_S of 3.19, would have made the cut of $J_S \geqslant 2$. It does not, however, show up in our source list.

The reduced χ^2 for the 6 light curves selected in the plot ranged from 1.72 to 2.24. There were some light curves with much lower values, but these were not considered good fits as the numerical fits came from spurious circumstance, *i.e.*, the time of maximum amplification being outside our observation window.

Method 2: Searching for Missed Sources

The source list obtained from DAOPHOT will miss some light sources. Sources

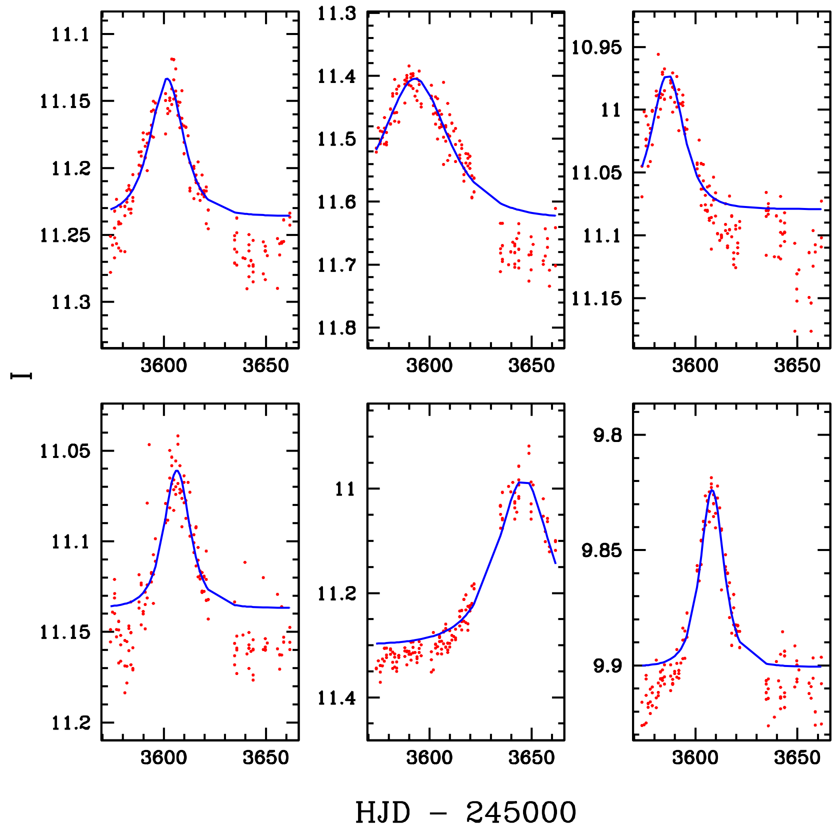

Fig. 5. Some of the light curves from our original source list which came closest to being well-fit by microlensing.

that are faint with respect to the background and have most or all of their brightening occur in frames which were not in the reference image will not make the list. We compiled a list of sources on the abs.fits image and removed those whose coordinate were within 1 pixel of sources already listed. 2 657 variable sources were added this way.

These sources were fit to microlensing curves using a Perl script. As only the differential flux was available, we modified the Paczyński equations for numerical convenience. Without blending and with knowledge of the base flux one would use:

$$U(t) = \sqrt{u_{\rm min}^2 + (\frac{t-t_o}{t_e^2})^2}, \tag{1}$$

$$A(t) = \frac{U^2+2}{U\sqrt{U^2+4}}. \tag{2}$$

Removing the base flux and solving for the variable flux:

$$\Delta F = \Delta F_{\max} G_{U_{\min}} \frac{U^2+2-U\sqrt{U^2+4}}{U\sqrt{U^2+4}} \tag{3}$$

where:

$$G_{U_{\min}} = \frac{u_{\min}\sqrt{u_{\min}^2+4}}{u_{\min}^2+2-U_{\min}\sqrt{u_{\min}^2+4}}. \tag{4}$$

Eq. (3) has the further advantage of being blending-independent (assuming non-variable blending). We did find a light curve corresponding to BLG-259, and with a $\chi^2 = 1.11$ it had one of the best fits. The light curves with an even lower χ^2 were either spurious *i.e.*, with huge errors or fewer data points, or they had their peak at the edge of our observational window.

We did not find any high-confidence, previously undetected microlensing candidates. We did however indirectly identify a similar light curve that is interesting in its own right. It was approximately symmetric, its time of maximum amplification was several days removed from the edges of our observation window, and its timescale was sufficiently short that a flat baseline is discernible; it is presented with its model fit in Fig. 6. The angular position of the event is $(\alpha,\delta) = (17^{\rm h}58^{\rm m}31^{\rm s}, -26^\circ54'43'')$. The closest object found in a Simbad search was IRAS-17554-2654 at a distance of $45''(\approx 3$ pixels), and it is classified as an "Infra-Red source", which is a magnitude 15 object at 12 μm. It is unfortunately not within sky regions covered by any OGLE field online. We also could not find a match in the ASAS catalog (Pojmański 1997). The reduced χ^2 for the fit is very high, 111.5. The best fit parameters were $(\Delta F_{\max}, u_{\min}, t_o, t_e) = (11720, 1.0, 3656.5, 3.14)$.

4.3. *Discussion*

One might ask what the purpose was of using two different methods, if the second method requires removing sources identified in the first method? We considered it valuable to compare different approaches. The first method, where its sources came from a DAOPHOT list obtained from the reference image, had the advantage that its relative fluxes on the difference images could be easily converted to magnitudes, as well as there being a large volume of proven software already designed for source identification. The second method has fewer biases preventing completeness, as variability does not need to occur within the frames used to construct the reference image. More empirical study is required to determine the optimal method studying microlensing curves that are entirely within the high-brightness domain.

The photometric capacity to refine parameters of known light curves is demonstrated by Figs. 3 and 4. The method we employed is not only effective at performing its task, but relatively easy to implement. Following proper reductions of the images, one need only feed ISIS a source list whose coordinates are obtained from the general surveys. The light curves can then be compared.

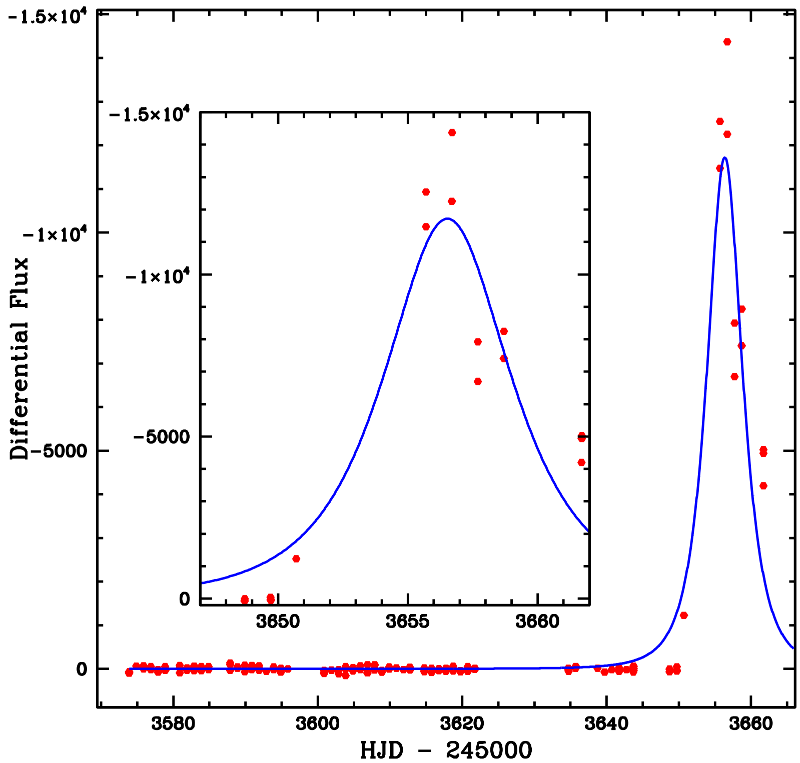

Fig. 6. An interesting light curve of unknown nature identified through a microlensing search. The fact the counts are negative is an artifact of the subtraction process, the event was in fact a brightening.

5. Other Variable Stars

Studies of variable stars towards the Galactic bulge have been a natural and important byproduct of microlensing surveys in that direction. For example, OGLE-II published a catalog of $\approx 200\,000$ variable stars discovered in the bulge during its first three years (Wozniak *et al.* 2002). Similarly, some 50 000 variable stars have been detected in that direction by the MACHO project (Cook *et al.* 1995). At brighter magnitudes, a survey with similar equipment to what we have used here – albeit also using a longer baseline and much higher cadence – would be very effective in identifying and classifying previously undiscovered variable stars.

With current data, we have light curves for $\approx 10^5$ sources, so we cannot match the sheer number of variable stars discovered by deeper microlensing surveys. We do however cover a different region of the parameter space: the brightest stars. We have nearly 800 sources brighter than magnitude 9, ≈ 5900 sources brighter than magnitude 10, and $\approx 32\,000$ sources brighter than magnitude 11.

We classify our variable stars into two groups: periodic and miscellaneous. Periodic variable stars were identified using an analysis of variance search developed by Schwarzenberg-Czerny (1989) and Devor (2005), as implemented by the VAR-

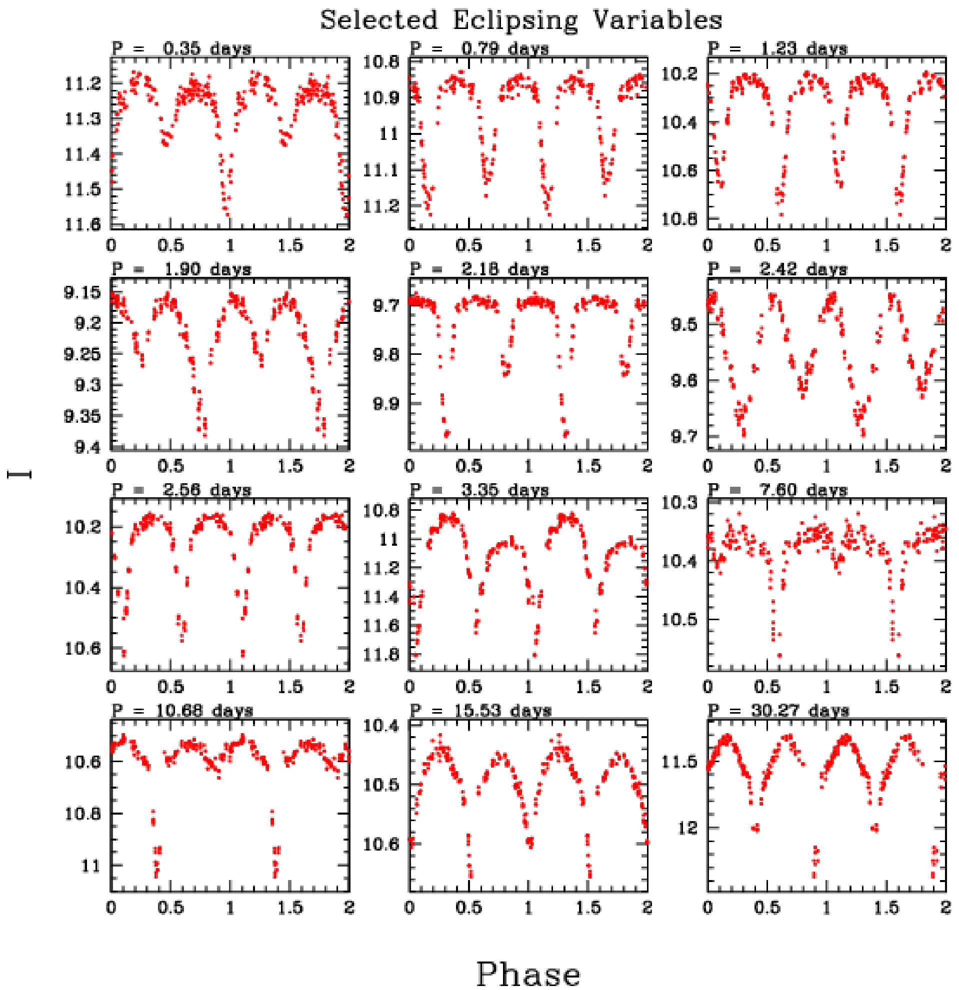

Fig. 7. Sample of 12 eclipsing variable stars.

TOOLS package for light curves (Hartman *et al.* 2008). On the 66 nights we have observations, the epochs came within a few tens of minutes of each other, so we effectively have 66 distinct points scattered erratically over the 88 night span of our observations. Aliasing was a significant issue in this domain, with most stars best-fit periods clustering in a small subset of frequency space, particularly the harmonics of 1 day. Fig. 7 is a sampling of some of the cleaner eclipsing variable stars we found in our data. Fig. 8 is in turn a sample of other periodic variable stars.

Within this sample alone and using a 30″ matching radius, we find 19 of the 36 variable sources shown here are without any match in Simbad. Expanding the matching radius to 45″ yields 4 additional matches. It is reasonable to estimate that around half or perhaps more of the variable stars which would show up in a more complete survey would constitute new discoveries. Further, many of the matches one would find are with the 2MASS catalog (Cutri *et al.* 2003) and the IRAS catalog

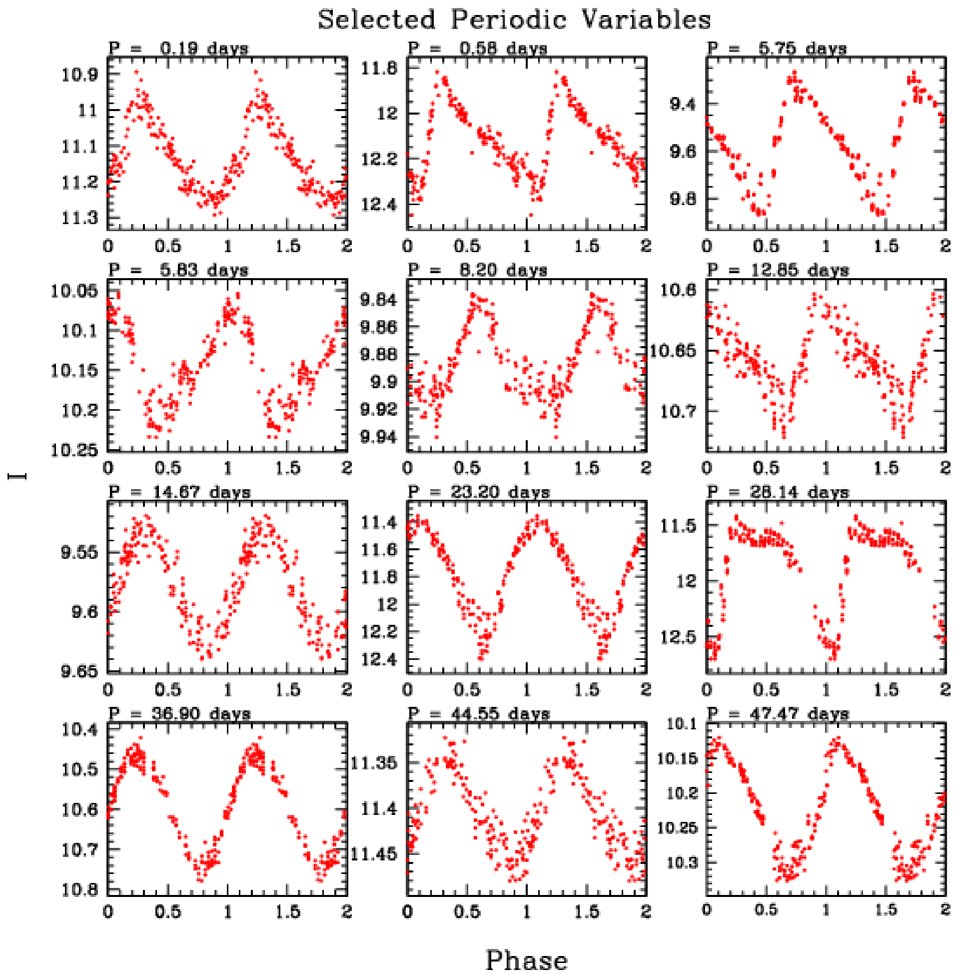

Fig. 8. Sample of 12 periodic variable stars.

(Kleinmann *et al.* 1986) and thus may contain incomplete variability information. The 7 matches we found in this manner with information on the period are from the General Catalog of Variable Stars (Kukarkin *et al.* 1971). We summarize those in Table 2. The ASAS catalog (Pojmański 1997) had matches to 6 of our 12 eclipsing variable stars and 7 of the 12 other periodic variable stars. As the ASAS and GCVS matches largely overlapped, this left 11 of the 24 sources selected without any match.

One eclipsing variable source standing out is the 3.35 day period eclipsing binary as it is demonstrating the O'Connell effect, a light curve asymmetry between outside eclipse maxima (see O'Connell 1951, Davidge and Milone 1984). We estimate the shift in brightness between maxima as $\Delta I \approx +0.2$ mag. Located at $(\alpha,\delta) = (18^{\mathrm{h}}24^{\mathrm{m}}29^{\mathrm{s}}, -32^\circ25'57'')$, it does have a $30''$ match with V* V3254 Sgr, which is listed as an eclipsing binary but without a period, without the O'Connell effect mentioned and a magnitude offset of ≈ 2.5.

Table 2

Periodic matches

Name	Archival Period	Measured Period	Class
V* BS Sco	7.622	7.60	EB (Algol)
V* V712 Sco	30.305	30.27	EB (Algol)
V* V3254 Sgr	–	3.35	EB (O'Connell)
V* V1188 Sgr	0.581	0.58	RR Lyr
V* V773 Sgr	5.748	5.75	δ Cep
V* V1828 Sgr	12.972	12.85	δ Cep
V* V1290 Sgr	27.9516	28.14	Cepheid

Periodic variable stars found to have matches in SIMBAD which include periodicity information. Periods are given in days.

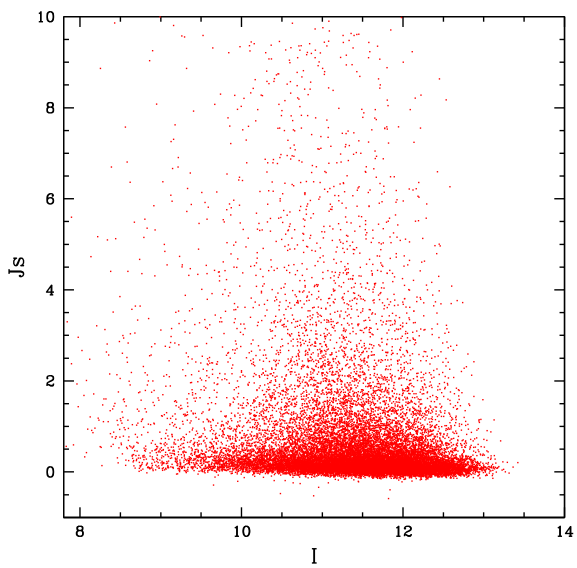

Fig. 9. Plot of Stetson's J index (J_S) of correlated variability *vs.* apparent magnitude in the *I*-band. A few more sources lie above the line $J_S = 10$.

To search for miscellaneous variable stars we apply a cut of $J_S > 0.85$, see Fig. 9. This selects 23 072 light curves as being candidate variable stars. There is nothing intrinsic about the value 0.85, it was chosen empirically to be where light curves began to appear unequivocally variable when the time series were viewed by eye. There likely were true variable stars below the cutoff, but we wanted to minimize the risk of false positives, and as such, sacrificed completeness. A plethora of

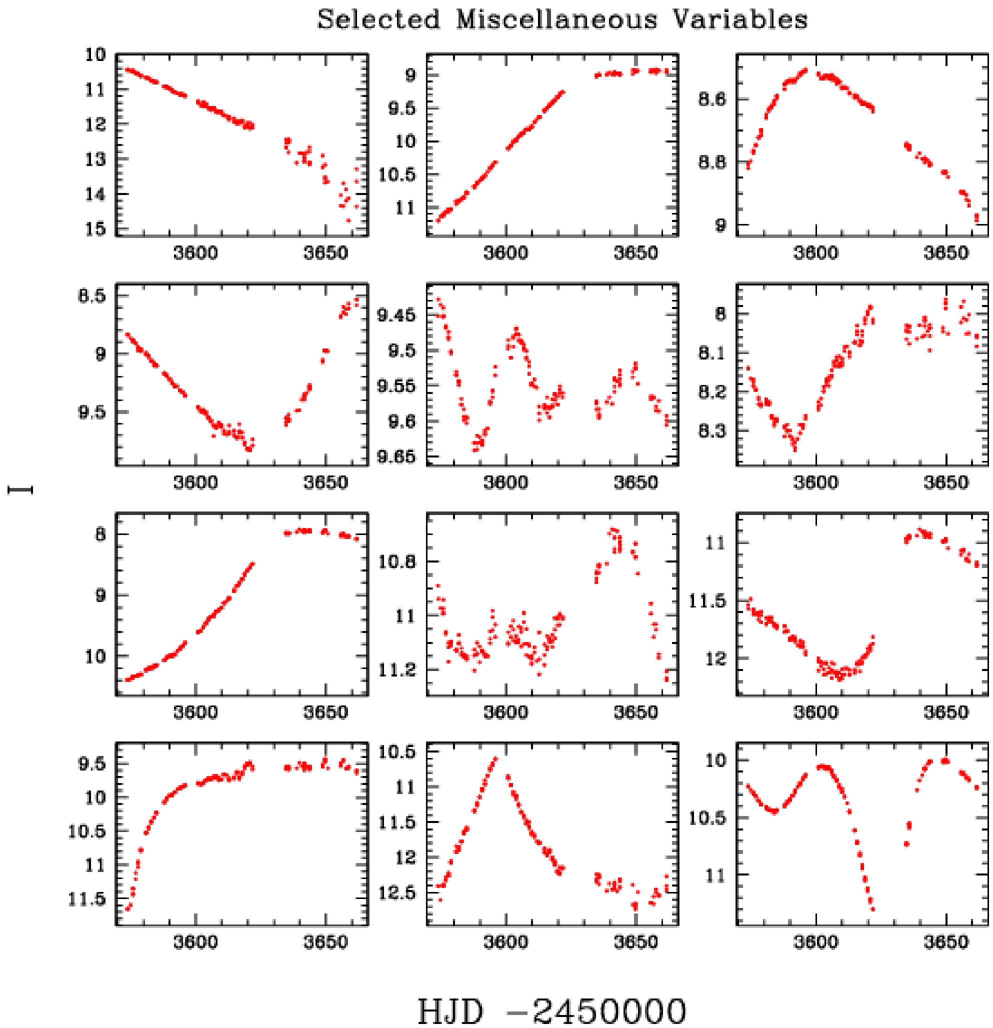

Fig. 10. Sample of 12 miscellaneous variable stars.

variable stars was available at all signal levels, with 9,775 sources having $J_S > 2.0$ and 1 264 having $J_S > 10.00$. Sources with a high J_S value but without a clear period numbered in the thousands. These were the variable sources we classified as miscellaneous. A selection is shown in Fig. 10. We had 30″ astrometric matches in SIMBAD for 9 of these but there was insufficient information to determine if they are all a correct match.

We choose not to use a larger matching radius for these sources as without a smoking gun (such as period) it is difficult to determine the validity of the match. For the 12th source, on the bottom right corner of Fig. 10, we find the classification scheme is in fact incorrect. Our match, V* V738 Sgr, is currently classified as a variable star of W Vir type with a period of 43.39 days (Kukarkin *et al.* 1971). We find that a 43.39 day period does not fit the light curve. We know that it is the same star as it is well fit by a period of $43.39 \times 2 = 86.78$ days. Further data would be required to confirm if this is indeed the correct period.

6. Conclusion

Using data from an imaging system with a wide FOV, fast focal ratio, and large pixel scale, combined with image subtraction photometry, we have found matches to seven OGLE microlensing events from the 2005 bulge season. We searched for previously undetected microlensing events using two distinct methods, fitting parameters to our DAOPHOT source list and fitting parameters to a new source list directly constructed from the difference images. We found a few events closely resembling microlensing events but none with a satisfactory fit. In a search for periodic variable stars we found that there are a great many high-brightness eclipsing and periodic variable stars still to be found in the bulge. A catalog of periodic variable stars based on the data discussed in this paper is in preparation (Nataf *et al.* 2009).

Buoyed by the proof-of-concept performance achieved here we encourage the development of Small Aperture Microlensing Survey (SAMS) – see Table 1. Such a suite of three small aperture telescopes equipped with high QE, large format CCD cameras would provide high sampling of the brightest bulge microlensing events along with a more complete catalog of bright bulge variable stars. This instrument would naturally be located in the Southern Hemisphere, and from the logistics point of view would probably be best located next to existing and planned larger aperture microlensing telescopes.

Acknowledgements. HATNet operations have been funded by NASA grants NEG04GN74G, NNX08AF23G and SAO IR&D grants. We thank J.D. Hartman for assistance with use of the VARTOOLS package, G. Pojmański for his LC program, W. Pych for his FWHM program, R.J. Siverd for explanations and help with Perl programming, S. Kozlowski for suggestions on microlensing fitting, Ł. Wyrzykowski for his microlensing curve fitting program, and A. Gould for insights into the observational process. We made use of the Simbad database, operated in Strasbourg, France by the Centre de Données astronomiques de Strasbourg.

REFERENCES

Alard, C. 2000, *A&AS*, **144**, 363.
Alard, C., and Lupton, R.H. 1998, *ApJ*, **503**, 325.
An, J.H., *et al.* 2002, *ApJ*, **572**, 521.
Bakos, G.A., Noyes, R.W., Kovacs, G., Stanek, K.Z., Sasselov, D.D., and Domsa, I. 2004, *PASP*, **116**, 266.
Bennett, D.P., and Rhie, S.H. 2000, *ASP Conf. Ser.*, **219**, 542.
Bennett, D.P., *et al.* 1993, *New York Academy Sciences Annals*, **688**, 612.
Bennett, D.P., *et al.* 2007, 2007arXiv0704.0454B.

Bond, I.A., *et al.* 2004, *ApJ*, **606**, 155.
Cook, K.H., *et al.* 1995, *ASP Conf. Ser.*, **83**, 221.
Crotts, A.P.S., and Tomaney, A.B. 1996, *ApJ*, **473**, 87.
Cutri, R.M., *et al.* 2003, "2MASS All Sky Catalog of point sources".
Darnley, M.J., *et al.* 2007, *ApJ*, **661**, 45.
Davidge, T.J., and Milone, E.F. 1984, *ApJS*, **55**, 571.
Devor, J. 2005, *ApJ*, **628**, 411.
Gaudi, B.S., *et al.* 2006, *Bull.A.A.S.*, **38**, 88.
Gaudi, B.S., *et al.* 2008, *Science*, **319**, 927.
Gaudi, B.S., *et al.* 2008, *ApJ*, **677**, 1268.
Gaudi, B.S., *et al.* 2009, *Astro2010: The Astronomy and Astrophysics Decadal Survey, Science White Papers*, **85**.
Gould, A. 1996, *ApJ*, **470**, 201.
Gould. A. 2008, in: "Manchester Microlensing Conference".
Gould, A. 2009, *ASP Conf. Ser.*, **403**, 86.
Gould, A., and Depoy, D.L. 1998, *ApJ*, **497**, 62.
Gould, A., *et al.* 2009, *ApJ*, **698**, 147.
Hartman, J.D., Bakos, G., Stanek, K.Z., and Noyes, R.W. 2004, *AJ*, **128**, 1761.
Hartman, J.D., Gaudi, B.S., Holman, M.J., McLeod, B.A., Stanek, K.Z., Barranco, J.A., Pinsonneault, M.H., and Kalirai, J.S. 2008, *ApJ*, **675**, 1254.
Johnson, J.A., Winn, J.N., Cabrera, N.E., and Carter, J.A. 2009, *ApJ*, **692**, 100.
Kleinmann, S.G., Cutri, R.M., Young, E.T., Low, F.J., and Gillett, F.C. 1997, VizieR Online Data Catalog.
Kukarkin, B.V., *et al.* 1971, "General Catalogue of Variable Stars", 3rd ed..
Lennon, D.J., Mao, S., Fuhrmann, K., and Gehren, T. 1996, *ApJ*, **471**, 23.
Novati, S. Calchi, *et al.* 2009, *ApJ*, **695**, 442.
O'Connell, D.J.K. 1951, *Publications of the Riverview College Observatory*, **2**, 85.
Paczyński, B. 1986, *ApJ*, **304**, 1.
Pojmański, G. 1997, *Acta Astron.*, **47**, 467.
Ramirez, S.V., Arendt, R.G., Sellgren, K., Stolovy, S.R., Cotera, A., Smith, H.A., and Yusef-Zadeh, F. 2008, *ApJS*, **175**, 147.
Sako, T., *et al.* 2008, *Experimental Astronomy*, **22**, 51.
Schwarzenberg-Czerny, A. 1989, *MNRAS*, **241**, 153.
Soszyński, I., Udalski, A., Szymański, M.K., Kubiak, M., Pietrzyński, G., Wyrzykowski, Ł., Szewczyk, O., Ulaczyk, K., and Poleski, R. 2008, *Acta Astron.*, **58**, 293.
Stetson, P.B. 1992, *Royal Astronomical Society of Canada, Journal*, **86**, 71.
Stetson, P.B. 1996, *PASP*, **108**, 851.
Szymański, M.K. 2005, *Acta Astron.*, **55**, 43.
Udalski, A. 2003, *Acta Astron.*, **53**, 291.
Udalski, A., Kubiak, M., and Szymański, M. 1997, *Acta Astron.*, **47**, 319.
Wozniak, P. R., Udalski, A., Szymański, M., Kubiak, M., Pietrzyński, G., Soszyński, I., and Żebruń, K. 2002, *Acta Astron.*, **52**, 129.
Wyrzykowski, Ł., *et al.* 2009, *MNRAS*, **397**, 1228.